AIMS Mathematics, 10(3): 6233–6257.
DOI: 10.3934/math.2025284
Received: 23 November 2024
Revised: 06 March 2025
Accepted: 11 March 2025
Published: 20 March 2025

https://www.aimspress.com/journal/Math

Research article

Chaos and hidden chaos in a 4D dynamical system using the fractal-fractional operators

A. E. Matouk[1,2,*]

[1] Department of Mathematics, College of Science Al-Zulfi, Majmaah University, Al-Majmaah, 11952, Saudi Arabia
[2] College of Engineering, Majmaah University, Al-Majmaah 11952, Saudi Arabia

***Correspondence:** Email: ae.mohamed@mu.edu.sa.

Abstract: Although fractional calculus is about three centuries old, it has become the key to understanding many complex real-world phenomena. During the past few decades, many fractional derivatives have appeared. Among these, the fractal-fractional derivatives have shown acceptance in describing some real-world problems. In this paper, the Caputo, Atangana-Baleanu, and Caputo-Fabrizio fractal-fractional operators were applied to generate complex dynamics in a 4D dynamical system. Some conditions for the exact solutions' existence and uniqueness were demonstrated when the fractal-fractional operators are implemented into the mentioned 4D dynamical system. Some Ulam-Hyers stability results were demonstrated in the indicated fractal-fractional systems. Computation processes were carried out to demonstrate some graphical results that showed the existence of several complex dynamics in the considered system as the fractal-fractional operators are implemented. Furthermore, the computations of the system's Lyapunov exponents and the bifurcation diagrams were used to illustrate the wide range of chaotic dynamics that exist in the considered fractal-fractional 4D system. Existence of hidden chaotic attractors were also found. This interesting dynamical phenomenon was validated by the bifurcation diagrams and basin set of attraction.

Keywords: fractal-fractional operators; a 4D dynamical system; chaos; Lyapunov exponents; hidden chaotic attractor
Mathematics Subject Classification: 34H10, 34C28, 37M05

1. Introduction

For more than three centuries, Leibniz and l'Hospital initiated the problem of fractional-order differentiation when they tried to generalize the calculus for integer order [1]. Afterwards, many fractional derivatives appeared such as the Caputo type [2], Caputo-Fabrizio type [3], and Atangana-Baleanu type [4]. They also provide better scenarios for understanding real-world phenomena.

Recently, the combination of the concept of fractional derivative and the concept of the fractal derivative set up the so-called fractal-fractional derivative (FFD) [5]. Thus, a new degree of freedom (the fractal parameter) appeared in the fractional operators, which makes them better candidate to handle the real-world problems. Therefore, some new FFDs have been developed such as the FFD in the Caputo sense, the FFD in the Atangana-Baleanu sense, and the FFD in the Caputo-Fabrizio sense.

Chaos theory was explored in many fields of science and engineering [6]. It can be used to precisely determine the unpredictable behaviors of dynamical systems. The chaotic dynamics can be verified by calculating the Lyapunov exponents (LEs) [7] and demonstrating the related bifurcation diagrams, which are considered effective means of clarifying the complex dynamics of the system. Some integer-order (IO) chaotic systems arising from science and engineering were reported such as the IO Lorenz system [8], the IO Rössler system [9], the IO modified autonomous Van der Pol- Duffing (ADVP) system [10] and the IO 4D dynamical system proposed by Matouk [11]. The fractional-order (FO) versions of the fore mentioned systems display chaotic dynamics such as the FO Lorenz system [12], the FO Rössler system [13], the FO modified ADVP system [14], and the FO 4D dynamical system proposed by Matouk [15]. The last FO system was represented by four equations with three quadratic terms. It is designed to display hyperchaotic attractors and also to feedback control one of its state variables. Therefore, it is suitable to display variety of chaotic and hyperchaotic dynamics.

On the other hand, mathematical modeling using the FFDs has recently become the focus of attention of scientists and researchers in various fields. In [16], Qureshi and Atangana designed a nonlinear epidemiological model based on the FFD in the Caputo sense. In [17], Sami et al. analyzed a food chain model under the FFD in the Caputo sense. In [18], Almutairi et al. discussed a pneumonia disease model under the FFD in the Atangana-Baleanu sense. In [19], Arif et al. investigated a fluid flow model using the FFD in the Caputo sense. In [20], Khan et al. studied a model for tuberculosis using the FFD. In [21], Shah and Abdeljawad studied a model of CO_2 emanations from energy sector using the FFD. Moreover, the FFDs show the effectiveness to generate chaotic attractors in dynamical systems. For example, Dlamini et al. demonstrated chaotic attractors in Lorenz system under the FFD in the Caputo-Fabrizio sense [22]. Ul Haq et al. investigated chaotic behaviors in a 3D dynamical system using the FFDs with exponential decay type kernels [23]. Saber succeeded to achieve chaos control in the Burke-Shaw system under the FFD in the Caputo-Fabrizio sense [24]. However, the LEs and bifurcation diagrams were not provided in any of the previous references.

The major contributions of this manuscript are outlined as follows: The Caputo, Atangana-Baleanu, and Caputo-Fabrizio fractal-fractional derivatives are applied to the mentioned 4D dynamical system. Then, the existence and uniqueness of the solutions of the resulting systems are proven based on Arzelá-Ascoli theorem and Schauder's fixed point lemma. Some Ulam-Hyers (U-H) stability results are proven in the indicated fractal-fractional systems. The simulation results show that the indicated fractal-fractional operators generate chaotic attractors and other complex dynamics in the considered 4D dynamical system. In addition, computations of the LEs, bifurcation diagrams and basin set of attraction are carried out to illustrate the wide range of chaotic dynamics and hidden chaos that exist in the considered 4D dynamical system. To the best of my knowledge, their implementation in fractal-

fractional systems is presented here for the first time.

The organization of this manuscript is outlined as follows: In Section 2, definitions of the FFDs are presented. In Section 3, the considered 4D dynamical system is described. In Section 4, the existence and uniqueness analysis of the considered 4D dynamical system involving the FFDs are carried out based on Arzelá-Ascoli theorem and Schauder's fixed point lemma. In Section 5, the systems' U-H stability analysis is discussed. In Section 6, numerical simulations of the considered 4D dynamical system under the FFDs are carried out. In Section 7, the conclusions are drawn.

2. Fractal-fractional calculus

First, we introduce the fractal-fractional integral operators (FFIOs) as follows [5]:

1) The ξ th-order FFIO with power law type kernel is given as

$$^{FFP}\mathrm{I}_{0,\tau}^{\xi,\eta}\left(\varphi(\tau)\right)=\eta[\int_{0}^{\tau}(\tau-x)^{\xi-1}x^{\eta-1}\varphi(x)dx]/\Gamma(\xi), \tag{1}$$

where $\varphi\in C(a,b),\xi>0,\eta\le m$ and $m\in N$.

2) The ξ th-order FFIO with exponentially decaying type kernel is given as

$$^{FFE}\mathrm{I}_{0,\tau}^{\xi,\eta}\left(\varphi(\tau)\right)=[\eta\xi\int_{0}^{\tau}x^{\eta-1}\varphi(x)dx+\eta(1-\xi)\tau^{\eta-1}\varphi(\tau)]/\mathrm{M}(\xi), \tag{2}$$

where $\varphi\in C(a,b)$, $\xi>0,\eta\le m,$ $m\in N$ and $\mathrm{M}(\xi)$ is a normalization function satisfying $\mathrm{M}(1)=\mathrm{M}(0)=1.$

3) The ξ th-order FFIO with Mittag-Leffler type kernel is given as

$$^{FFM}\mathrm{I}_{0,\tau}^{\xi,\eta}\left(\varphi(\tau)\right)=[\eta\xi\int_{0}^{\tau}x^{\eta-1}\varphi(x)(\tau-x)^{\xi-1}dx+\eta(1-\xi)\tau^{\eta-1}\varphi(\tau)]/\mathrm{AB}(\xi), \tag{3}$$

where $\varphi\in C(a,b),$ $\xi>0,\eta\le m,$ $m\in N$ and $\mathrm{AB}(\xi)=\dfrac{\xi}{\Gamma(\xi)}+1-\xi.$

Assume that $l=ceil(\xi)\in N,\eta\in(l-1,l)$. Hence, according to the above-mentioned FFIO, the following FFDs [5] are defined as

I) The ξ th-order FFD with power law type kernel is given as

$$^{FFP}D_{0,\tau}^{\xi,\eta}\left(\varphi(\tau)\right)=\frac{d}{d\tau^{\eta}}[\int_{0}^{\tau}(\tau-x)^{l-\xi-1}\varphi(x)dx]/\Gamma(l-\xi), \tag{4}$$

where $\dfrac{d\varphi(\tau)}{d\tau^{\eta}}=\lim_{t\to\tau}\dfrac{\varphi(t)-\varphi(\tau)}{t^{\eta}-\tau^{\eta}}.$ This type of FFDs is also called fractal-fractional Caputo (FF-C) derivative.

II) The ξ th-order FFD with exponentially decaying type kernel is given as

$$^{FFE}D_{0,\tau}^{\xi,\eta}\left(\varphi(\tau)\right)=[\mathrm{M}(\xi)\frac{d}{d\tau^{\eta}}\int_{0}^{\tau}\exp\left(-\frac{\xi}{1-\xi}(\tau-x)\right)\varphi(x)dx]/(1-\xi). \tag{5}$$

This FFD is also called fractal-fractional Caputo-Fabrizio (FF-CF) derivative.

III) The ξ th-order FFD with Mittag-Leffler type kernel is given as

$$^{FFM}D_{0,\tau}^{\xi,\eta}\left(\varphi(\tau)\right)=[\mathrm{AB}(\xi)\frac{d}{d\tau^{\eta}}\int_{0}^{\tau}\mathrm{E}_{\xi}\left[-\frac{\xi}{1-\xi}(\tau-x)^{\xi}\right]\varphi(x)dx]/(1-\xi), \tag{6}$$

where $0<\xi,\eta\leq 1$ and $\mathrm{E}_{\xi}(.)$ represents the Mittag-Leffler function. The operator $^{FFM}D_{0,\tau}^{\xi,\eta}$ is also equivalent to the Atangana-Baleanu FFD of the Caputo sense, or simply $^{FF-ABC}D_{0,\tau}^{\xi,\eta}$. Hence, the corresponding FFIO is

$$^{FFM}\mathrm{I}_{0,\tau}^{\xi,\eta}\left(\varphi(\tau)\right)=[\frac{\eta\xi}{\Gamma(\xi)}\int_{0}^{\tau}x^{\eta-1}\varphi(x)(\tau-x)^{\xi-1}dx+\eta(1-\xi)\tau^{\eta-1}\varphi(\tau)]/\mathrm{M}(\xi). \tag{7}$$

To conclude this, the FFD-ABC is denoted by

$$^{FF-ABC}D_{0,\tau}^{\xi,\eta}\left(\varphi(\tau)\right)=[\mathrm{AB}(\xi)\frac{d}{d\tau^{\eta}}\int_{0}^{\tau}\mathrm{E}_{\xi}\left[-\frac{\xi}{1-\xi}(\tau-x)^{\xi}\right]\varphi(x)dx]/(1-\xi). \tag{8}$$

The FFD-C is denoted by

$$^{FF-C}D_{0,\tau}^{\xi,\eta}\left(\varphi(\tau)\right)=\frac{d}{d\tau^{\eta}}[\int_{0}^{\tau}(\tau-x)^{l-\xi-1}\varphi(x)dx]/\Gamma(l-\xi). \tag{9}$$

The FF-CF is denoted by

$$^{FF-CF}D_{0,\tau}^{\xi,\eta}\left(\varphi(\tau)\right)=[\mathrm{M}(\xi)\frac{d}{d\tau^{\eta}}\int_{0}^{\tau}\exp\left(-\frac{\xi}{1-\xi}(\tau-x)\right)\varphi(x)dx]/(1-\xi). \tag{10}$$

3. The 4D dynamical system

The 4D dynamical system given by Matouk [11] was first introduced in terms of ODEs as follows:

$$\begin{aligned}
d\rho_1/d\tau&=\alpha'(\rho_4-\rho_2)+\nu'\rho_1-\rho_1\rho_4,\\
d\rho_2/d\tau&=\beta'\rho_1+\rho_4-\rho_1\rho_3,\\
d\rho_3/d\tau&=\rho_1^2-\sigma'\rho_3,\\
d\rho_4/d\tau&=\delta'\rho_4.
\end{aligned} \tag{11}$$

The system's parameters are $\alpha',\beta',\delta',\nu',\sigma'\in R$. System (11) displays chaotic dynamics when $\alpha'=-3,\beta'=15,\delta'=-0.0001,\nu'=-1.5,\sigma'=0.6.$ The physical meaning of these parameters can be

realized form the following circuital equations that relate to system (11):

$$d\rho_1/d\tau = -\frac{1}{R_2C_1}\rho_4 + \frac{1}{R_3C_1}\rho_2 - \frac{1}{R_4C_1}\rho_1 - \frac{1}{R_1C_1}\rho_1\rho_4,$$
$$d\rho_2/d\tau = \frac{1}{R_7C_2}\rho_1 + \frac{1}{R_6C_2}\rho_4 - \frac{1}{R_5C_2}\rho_1\rho_3,$$
$$d\rho_3/d\tau = \frac{1}{R_8C_3}\rho_1^2 - \frac{1}{R_9C_3}\rho_3,$$
$$d\rho_4/d\tau = -\frac{1}{R_{10}C_4}\rho_4,$$

where $R_1 = R_5 = R_6 = R_8 = 1k\Omega,\ R_2 = R_3 = 0.3333k\Omega,\ R_4 = 0.6667k\Omega, R_7 = 0.0667k\Omega, R_8 = 1k\Omega,$ $R_9 = 1.6667k\Omega, R_{10} = 10000k\Omega$ and $C_i = 10nF,\ i = 1,2,3,4.$ System (11) has three equilibria as follows:

$$\mathrm{P}_0 = (0,0,0,0),\ \mathrm{P}_1' = (\lambda', \frac{\lambda'\nu'}{\alpha'}, \beta', 0),\ \mathrm{P}_2' = (-\lambda', -\frac{\lambda'\nu'}{\alpha'}, \beta', 0),\ \lambda' = \sqrt{\beta'\sigma'}.$$

The equilibrium P_0 is a saddle point when $\nu' < 0$ and $\alpha'\beta' < 0$ since it has the eigenvalues:

$$\Lambda_1' = \delta', \Lambda_2' = -\sigma' \quad \text{and} \quad \Lambda_{3,4}' = \frac{\nu' \pm \sqrt{(\nu')^2 - 4\alpha'\beta'}}{2}.$$

Then, we replace the integer-order derivatives with FFDs as follows:

$$^{FF}D_{0,\tau}^{\xi,\eta}\rho_1(\tau) = \alpha'(\rho_4 - \rho_2) + \nu'\rho_1 - \rho_1\rho_4,$$
$$^{FF}D_{0,\tau}^{\xi,\eta}\rho_2(\tau) = \beta'\rho_1 + \rho_4 - \rho_1\rho_3,$$
$$^{FF}D_{0,\tau}^{\xi,\eta}\rho_3(\tau) = \rho_1^2 - \sigma'\rho_3,$$
$$^{FF}D_{0,\tau}^{\xi,\eta}\rho_4(\tau) = \delta'\rho_4,$$

where $^{FF}D_{0,\tau}^{\xi,\eta}$ refers to an arbitrary FFD. Obviously, the RHS of last fractal-fractional system has the dimension of $\frac{1}{time}$. Hence, to avoid dimensional discrepancy, one sets

$$^{FF}D_{0,\tau}^{\xi,\eta}\rho_1(\tau) = \alpha(\rho_4 - \rho_2) + \nu\rho_1 - \rho_1\rho_4,$$
$$^{FF}D_{0,\tau}^{\xi,\eta}\rho_2(\tau) = \beta\rho_1 + \rho_4 - \rho_1\rho_3,$$
$$^{FF}D_{0,\tau}^{\xi,\eta}\rho_3(\tau) = \rho_1^2 - \sigma\rho_3,$$
$$^{FF}D_{0,\tau}^{\xi,\eta}\rho_4(\tau) = \delta\rho_4,$$

where $\alpha = \alpha'(\eta,\xi), \beta = \beta'(\eta,\xi), \delta = \delta'(\eta,\xi), \nu = \nu'(\eta,\xi), \sigma = \sigma'(\eta,\xi).$ This system has three equilibria as follows:

$$\mathrm{P}_0 = (0,0,0,0),\ \mathrm{P}_1 = (\lambda, \frac{\lambda\nu}{\alpha}, \beta, 0),\ \mathrm{P}_2 = (-\lambda, -\frac{\lambda\nu}{\alpha}, \beta, 0),\ \lambda = \sqrt{\beta\sigma}.$$

Here, motivated by the previous discussion, P_0 can be a saddle point under specific selections of the system's parameters $\alpha, \beta, \delta, \nu, \sigma$, the fractal dimension η, and the fractional parameter ξ. In addition, any equilibrium point P_i, $i = 1,2$ is locally asymptotically stable (LAS) if Λ is a negative real number, where Λ is an arbitrary eigenvalue of the linearized part of the above-mentioned fractal-fractional system.

4. Existence and uniqueness analysis of the 4D dynamical system under the FFDs

System (11), using the operator ${}^{FF-ABC}D_{0,\tau}^{\xi,\eta}$, can be formulated as

$$\begin{aligned}
{}^{FF-ABC}D_{0,\tau}^{\xi,\eta}\rho_1 &= \eta\tau^{\eta-1}\chi_1(\rho_1,\rho_2,\rho_3,\rho_4),\\
{}^{FF-ABC}D_{0,\tau}^{\xi,\eta}\rho_2 &= \eta\tau^{\eta-1}\chi_2(\rho_1,\rho_2,\rho_3,\rho_4),\\
{}^{FF-ABC}D_{0,\tau}^{\xi,\eta}\rho_3 &= \eta\tau^{\eta-1}\chi_3(\rho_1,\rho_2,\rho_3,\rho_4),\\
{}^{FF-ABC}D_{0,\tau}^{\xi,\eta}\rho_4 &= \eta\tau^{\eta-1}\chi_4(\rho_1,\rho_2,\rho_3,\rho_4).
\end{aligned} \tag{12}$$

System (12) can also be rewritten in general form as

$$\begin{cases}
{}^{FF-ABC}D_{0,\tau}^{\xi,\eta}\mathrm{X}(\tau) = \eta\tau^{\eta-1}\Psi(\tau,\mathrm{X}(\tau)), \quad \tau \geq 0,\\
\mathrm{X}(0) = \mathrm{X}_0.
\end{cases} \tag{13}$$

Applying the FFIO (3), one gets

$$\mathrm{X}(\tau) - \mathrm{X}(0) = \frac{\xi\eta}{\mathrm{M}(\xi)\Gamma(\xi)}\int_0^\tau x^{\eta-1}\Psi(x,\mathrm{X}(x))(\tau-x)^{\xi-1}dx + \frac{\eta(1-\xi)\tau^{\eta-1}\Psi(\tau,\mathrm{X}(\tau))}{\mathrm{M}(\xi)}. \tag{14}$$

Then, the norm $\|\mathrm{X}\| = \max_{\tau\in[0,T]}\left|\sum_{i=1}^{4}\rho_i(\tau)\right|$ is defined in the Banach space $\mathrm{B} = \Phi\times\Phi\times\Phi\times\Phi$, such that $\Phi = C[0,T]$. Hence, the operator $J:\mathrm{B}\to\mathrm{B}$ is defined as follows:

$$J\mathrm{X}(\tau) = \mathrm{X}(0) + \frac{\xi\eta}{\mathrm{M}(\xi)\Gamma(\xi)}\int_0^\tau x^{\eta-1}\Psi(x,\mathrm{X}(x))(\tau-x)^{\xi-1}dx + \frac{\eta(1-\xi)\tau^{\eta-1}\Psi(\tau,\mathrm{X}(\tau))}{\mathrm{M}(\xi)}. \tag{15}$$

We consider the following Lipschitz hypotheses:

C1: $\forall \mathrm{X}\in\mathrm{B}, \exists L>0$ and L_a S.T. $\left|\Psi(\tau,\mathrm{X}(\tau))\right| \leq L\left|\mathrm{X}(\tau)\right| + L_a$, where L and L_a are constants.

C2: $\forall \mathrm{X}, \mathrm{X}_a \in \mathrm{B}, \exists L_a > 0$ S.T. $\left|\Psi(\tau,\mathrm{X}(\tau)) - \Psi(\tau,\mathrm{X}_a(\tau))\right| \leq L_a\left|\mathrm{X}(\tau) - \mathrm{X}_a(\tau)\right|$, where L_a is a constant.

C3: $\forall \mathrm{X}, \mathrm{X}_a \in \mathrm{B}, \exists L_a > 0$ S.T. $\left|\Psi(\tau,\mathrm{X}(\tau)) - \Psi(\tau,\mathrm{X}_a(\tau))\right| \leq L_a\left|\mathrm{X}(\tau)\right| - \left|\mathrm{X}_a(\tau)\right|$, where L_a is a constant.

Now, we present the following existence theorem:

Theorem 1. Suppose that C1 holds. If there exists a continuous function $\Lambda:[0,T]\times \mathrm{B}\to R,$ then at least one solution must exist for system (12).

Proof. One first defines the set $\Theta=\{\mathrm{X}\in \mathrm{B}:\|\mathrm{X}\|\le \varepsilon,\ \varepsilon\in R^{+}\}.$ Hence, using the assumption $\mathrm{X}\in \mathrm{B},$ one gets

$$\begin{aligned}\|J\mathrm{X}\| &= \max_{\tau\in[0,T]}\left|\mathrm{X}(0)+\frac{\eta\tau^{\eta-1}(1-\xi)}{\mathrm{M}(\xi)}\Psi(\tau,\mathrm{X}(\tau))+\frac{\xi\eta}{\mathrm{M}(\xi)\Gamma(\xi)}\int_0^{\tau}x^{\eta-1}\Psi(x,\mathrm{X}(x))(\tau-x)^{\xi-1}dx\right|\\ &\le \mathrm{X}(0)+\frac{\eta\tau^{\eta-1}(1-\xi)}{\mathrm{M}(\xi)}[L\|\mathrm{X}\|+L_a]+\max_{\tau\in[0,T]}\frac{\xi\eta}{\mathrm{M}(\xi)\Gamma(\xi)}\int_0^{\tau}x^{\eta-1}(\tau-x)^{\xi-1}\left|\Psi(x,\mathrm{X}(x))\right|dx\\ &\le \mathrm{X}(0)+\frac{\eta\tau^{\eta-1}(1-\xi)}{\mathrm{M}(\xi)}[L\|\mathrm{X}\|+L_a]+\frac{\xi\eta}{\mathrm{M}(\xi)\Gamma(\xi)}[L\|\mathrm{X}\|+L_a]\tau^{\xi+\eta-1}\beta(\xi,\eta)\le R,\end{aligned}$$

where $\beta(\xi,\eta)$ refers to the beta function. Consequently, it has been proven that J is uniformly bounded. In addition, one gets

$$\begin{aligned}\|J\mathrm{X}(\tau_2)-J\mathrm{X}_a(\tau_1)\| &= \max_{\tau\in[0,T]}\left|\frac{\eta\tau_2^{\eta-1}(1-\xi)}{\mathrm{M}(\xi)}\Psi(\tau_2,\mathrm{X}(\tau_2))+\frac{\xi\eta}{\mathrm{M}(\xi)\Gamma(\xi)}\int_0^{\tau_2}x^{\eta-1}\Psi(x,\mathrm{X}(x))(\tau_2-x)^{\xi-1}dx\right.\\ &\quad\left.-\frac{\eta\tau_1^{\eta-1}(1-\xi)}{\mathrm{M}(\xi)}\Psi(\tau_1,\mathrm{X}(\tau_1))-\frac{\xi\eta}{\mathrm{M}(\xi)\Gamma(\xi)}\int_0^{\tau_1}x^{\eta-1}\Psi(x,\mathrm{X}(x))(\tau_1-x)^{\xi-1}dx\right|\\ &\le \frac{\eta\tau_1^{\eta-1}(1-\xi)}{\mathrm{M}(\xi)}[L\|\mathrm{X}\|+L_a]+\frac{\xi\eta}{\mathrm{M}(\xi)\Gamma(\xi)}[L\|\mathrm{X}\|+L_a]\tau_1^{\xi+\eta-1}\beta(\xi,\eta)\\ &\quad-\frac{\eta\tau_2^{\eta-1}(1-\xi)}{\mathrm{M}(\xi)}[L\|\mathrm{X}\|+L_a]-\frac{\xi\eta}{\mathrm{M}(\xi)\Gamma(\xi)}[L\|\mathrm{X}\|+L_a]\tau_2^{\xi+\eta-1}\beta(\xi,\eta).\end{aligned}$$

Obviously, $\|J\mathrm{X}(\tau_2)-J\mathrm{X}_a(\tau_1)\|\to 0$ as $\tau_2\to\tau_1,$ which means that the operator J is equi-continuous. Thus, based on the Arzelá-Ascoli theorem, operator J is completely continuous. Then, according to the Schauder's fixed point lemma [25], it is clear that the solution of system (12) exists.

To discuss the uniqueness of the solution, one presents the following theorem:

Theorem 2. Suppose that C2 holds. System (12) has a unique solution if $\mathrm{K}<1,$ where

$$\mathrm{K}=\left[\frac{\eta T^{\eta-1}(1-\xi)}{\mathrm{M}(\xi)}+\frac{\xi\eta T^{\xi+\eta-1}}{\mathrm{M}(\xi)\Gamma(\xi)}\beta(\xi,\eta)\right]L_a. \tag{16}$$

Proof. Assume that $\mathrm{X},\mathrm{X}_a\in \mathrm{B},$ one gets

$$\|J\mathrm{X}-J\mathrm{X}_a\|=\max_{\tau\in[0,T]}\left|\frac{\eta\tau^{\eta-1}(1-\xi)}{\mathrm{M}(\xi)}[\Psi(\tau,\mathrm{X}(\tau))-\Psi(\tau,\mathrm{X}_a(\tau))]+\frac{\xi\eta}{\mathrm{M}(\xi)\Gamma(\xi)}\int_0^{\tau}x^{\eta-1}(\tau-x)^{\xi-1}[\Psi(x,\mathrm{X}(x))-\Psi(x,\mathrm{X}_a(x))]dx\right|$$

$$\le\left(\frac{\eta T^{\eta-1}(1-\xi)}{\mathrm{M}(\xi)}+\frac{\xi\eta T^{\xi+\eta-1}}{\mathrm{M}(\xi)\Gamma(\xi)}\beta(\xi,\eta)\right)\|\mathrm{X}-\mathrm{X}_a\|.$$

Thus, J has been shown to be a contraction mapping. According to the Banach contraction principle, it has been proven that system (12) has a unique solution.

To discuss the existence and uniqueness for the solutions of system (11) using the FF-C derivative, one writes the system as follows:

$$\begin{cases} {}^{FFC}D_{0,\tau}^{\xi,\eta}\mathrm{X}(\tau) = \eta\tau^{\eta-1}\Psi(\tau,\mathrm{X}(\tau)), \quad \tau \geq 0,\ 0 < \xi,\eta \leq 1, \\ \mathrm{X}(0) = \mathrm{X}_0. \end{cases} \tag{17}$$

Applying fractional integral (1), one gets

$$\mathrm{X}(\tau) = \mathrm{X}(0) + \frac{\eta}{\Gamma(\xi)}\int_0^\tau x^{\eta-1}\Psi(x,\mathrm{X}(x))(\tau-x)^{\xi-1}dx. \tag{18}$$

Hence, the operator $J:\mathrm{B}\to\mathrm{B}$ is defined as follows:

$$J\mathrm{X}(\tau) = \mathrm{X}(0) + \frac{\eta}{\Gamma(\xi)}\int_0^\tau x^{\eta-1}\Psi(x,\mathrm{X}(x))(\tau-x)^{\xi-1}dx. \tag{19}$$

Therefore, based on the fixed point theory [25], the following theorem holds.

Theorem 3. Assume that $J:\mathrm{B}\to\mathrm{B},$ is a fully-continuous mapping. As $\Xi(J) = \{\mathrm{X}\in\mathrm{B}:\mathrm{X} = tJ(\mathrm{X}), t\in(0,1)\}$ is bounded, the operator J defined in Eq (19) has at least a fixed point in B.

Theorem 4. Suppose that $\Psi:[0,T]\times\mathrm{B}\to R$ is a continuous function, then the operator J shows the compactness.

Proof. One first defines the set $\Theta_\Psi = \{\forall\mathrm{X}\in\mathrm{B}\exists L_\Psi\in R^+:|\Psi(\tau,\mathrm{X}(\tau))|\leq L_\Psi\}\subset\mathrm{B}$. Hence, when $\mathrm{X}\in\Theta_\Psi,$ one gets

$$\begin{aligned} \|J\mathrm{X}\| &= \frac{\eta L_\Psi}{\Gamma(\xi)}\max_{\tau\in[0,T]}\left|\int_0^\tau x^{\eta-1}(\tau-x)^{\xi-1}dx\right| \\ &\leq \frac{\eta L_\Psi T^{\xi+\eta-1}}{\Gamma(\xi)}\beta(\xi,\eta). \end{aligned} \tag{20}$$

Consequently, it has been proven that J is uniformly bounded. Moreover, for every $\tau_1,\tau_2\in[0,T]$ and $\mathrm{X}\in\mathrm{B},$ one gets

$$\begin{aligned} \|J\mathrm{X}(\tau_2) - J\mathrm{X}(\tau_1)\| &= \frac{\eta L_\mathrm{X}}{\Gamma(\xi)}\max_{\tau\in[0,T]}\left|\int_0^{\tau_2} x^{\eta-1}(\tau_2-x)^{\xi-1}dx - \int_0^{\tau_1} x^{\eta-1}(\tau_1-x)^{\xi-1}dx\right| \\ &\leq \frac{\eta L_\mathrm{X}\beta(\xi,\eta)}{\Gamma(\xi)}[\tau_2^{\xi+\eta-1} - \tau_1^{\xi+\eta-1}]. \end{aligned} \tag{21}$$

Clearly, $\|J\mathrm{X}(\tau_2) - J\mathrm{X}(\tau_1)\|\to 0$ as $\tau_2\to\tau_1$, which implies that the operator J is equi-continuous. Thus, J is bounded and continuous as well. Then, according to the Arzelá-Ascoli theorem, operator J is relatively-compact, which implies that J is completely continuous. Therefore, according to the Schauder's fixed point lemma, it has been proven that the solution of system (17) exists.

The uniqueness of the solution of system (17) is proved as follows:

Theorem 5. Suppose that C3 holds. System (17) has a unique solution if $\mathrm{K}' < 1$, where

$$\mathrm{K}' = \frac{\eta L_a T^{\xi+\eta-1}\beta(\xi,\eta)}{\Gamma(\xi)}. \tag{22}$$

Proof. Let $\max_{\tau\in(0,T)}|\Psi(\tau,0)| = \mathrm{Y}_a < \infty$, S.T. $\frac{\eta T^{\xi+\eta-1}\beta(\xi,\eta)\mathrm{Y}_a}{\Gamma(\xi)-\eta T^{\xi+\eta-1}\beta(\xi,\eta)L_a} \le r$. Then, one defines $\Delta_r = \{\mathrm{X}\in \mathrm{Y} : \|\mathrm{X}\| \le r\}$. Hence, one gets

$$\begin{aligned}
\|J\mathrm{X}\| &= \frac{\eta}{\Gamma(\xi,\theta)}\max_{\tau\in(0,T)}\int_0^\tau x^{\eta-1}(\tau-x)^{\xi-1}\big[|\Psi(\tau,\mathrm{X}(\tau))-\Psi(\tau,0)|+|\Psi(\tau,0)|\big]dx\\
&\le \frac{\eta T^{\xi+\eta-1}\beta(\xi,\eta)}{\Gamma(\xi)}\big(L_a\|\mathrm{X}\|+\mathrm{Y}_a\big)\\
&\le \frac{\eta T^{\xi+\eta-1}\beta(\xi,\eta)}{\Gamma(\xi)}\big(L_a r+\mathrm{Y}_a\big)\\
&\le r.
\end{aligned}$$

Thus, $J(\mathrm{X})\subset\Delta_r$. Based on (19) and the condition C3, it is found that

$$\begin{aligned}
\|J\mathrm{X}-J\mathrm{X}_a\| &= \frac{\eta}{\Gamma(\xi)}\max_{\tau\in(0,T)}\left|\int_0^\tau [x^{\eta-1}(\tau-x)^{\xi-1}\Psi(x,\mathrm{X}(x))-x^{\eta-1}(\tau-x)^{\xi-1}\Psi(x,\mathrm{X}_a(x))]dx\right|\\
&\le \mathrm{K}'\|\mathrm{X}-\mathrm{X}_a\|.
\end{aligned}$$

Hence, J has been shown to be a contraction mapping. Therefore, the Banach contraction principle implies that system (17) has a unique solution.

Finally, system (11) using the FF-CF derivative can be formulated as

$$\begin{cases} {}^{FF-CF}D_{0,\tau}^{\xi,\eta}\mathrm{X}(\tau) = \eta\tau^{\eta-1}\Psi(\tau,\mathrm{X}(\tau)), \quad \tau\ge 0,\ 0<\xi,\eta\le 1,\\ \mathrm{X}(0)=\mathrm{X}_0. \end{cases} \tag{23}$$

The existence of a unique solution of system (23) can be obtained via similar analysis.

5. U-H stability

In this section, a small perturbation $\delta(\tau)\in C[0,T]$, which is only dependent on $\delta(0)=0$, is considered. Furthermore,

$\delta(\tau)\le\varepsilon$ for $\varepsilon>0$,

${}^{FF}D_{0,\tau}^{\xi,\eta}\mathrm{X}(\tau) = \Psi(\tau,\mathrm{X}(\tau))+\delta(\tau)$.

Definition 1. A system governed by the FFD is U-H stable if $\exists \mathrm{N}_{\xi,\eta}\ge 0$ S.T. for any $\varepsilon>0$ and $\forall \mathrm{X}\in(C[0,T],R)$ fulfils the following inequality:

$$\left|{}^{FF}D_{0,\tau}^{\xi,\eta}\left(\mathrm{X}(\tau)\right)-\Psi(\tau,\mathrm{X}(\tau))\right|\leq\varepsilon,\tau\in[0,T],$$

and there exists a unique solution $Z\in(C[0,T],R)$ such that $\left|\mathrm{X}(\tau)-Z(\tau)\right|\leq\varepsilon\mathrm{N}_{\xi,\eta}$, $0\leq\tau\leq T$.

Consider the following perturbed solution of system (12):

$$\begin{cases}{}^{FFM}D_{0,\tau}^{\xi,\eta}\mathrm{X}(\tau)=\Psi(\tau,\mathrm{X}(\tau))+\delta(\tau), & \tau\geq 0,\\ \mathrm{X}(0)=\mathrm{X}_0,\end{cases}\tag{24}$$

where $\delta(\tau)\in C[0,T]$.

Based on hypothesis C2 and the above-mentioned analysis, system (24) fulfils the following inequality:

$$\left|\mathrm{N}(\tau)-\left(\mathrm{X}(0)+\frac{\xi\eta}{\mathrm{AB}(\xi)\Gamma(\xi)}\int_0^\tau x^{\eta-1}\Psi(x,\mathrm{X}(x))(\tau-x)^{\eta-1}dx+\frac{\eta(1-\xi)\tau^{\eta-1}\Psi(\tau,\mathrm{X}(\tau))}{\mathrm{AB}(\xi)}\right)\right|\leq\varepsilon\xi_{\xi,\eta}^{*},\tag{25}$$

where

$$\xi_{\xi,\eta}^{*}=\frac{\eta T^{\eta-1}(1-\xi)}{\mathrm{AB}(\xi)}+\frac{\xi\eta T^{\xi+\eta-1}}{\mathrm{AB}(\xi)\Gamma(\xi)}\beta(\xi,\eta).$$

Lemma 1. The solution of system (12) is U-H stable if $\mathrm{K}<1$, and the inequality (25) holds.

Proof. Suppose that $\mathrm{X},\mathrm{Z}\in\mathrm{B}$ and the solution X is unique.

$$\begin{aligned}&\left|\mathrm{X}(\tau)-\mathrm{Z}(\tau)\right|=\\&\left|\mathrm{X}(\tau)-\left(\mathrm{Z}(0)+\frac{\xi\eta}{\mathrm{AB}(\xi)\Gamma(\xi)}\int_0^\tau x^{\eta-1}\Psi(x,\mathrm{Z}(x))(\tau-x)^{\eta-1}dx+\frac{\eta(1-\xi)\tau^{\eta-1}\Psi(\tau,\mathrm{Z}(\tau))}{\mathrm{AB}(\xi)}\right)\right|\\&\leq\left|\mathrm{X}(\tau)-\left(\mathrm{Z}(0)+\frac{\xi\eta}{\mathrm{AB}(\xi)\Gamma(\xi)}\int_0^\tau x^{\eta-1}\Psi(x,\mathrm{X}(x))(\tau-x)^{\eta-1}dx+\frac{\eta(1-\xi)\tau^{\eta-1}\Psi(\tau,\mathrm{X}(\tau))}{\mathrm{AB}(\xi)}\right)\right|\\&+\left|\mathrm{X}(0)+\frac{\xi\eta}{\mathrm{AB}(\xi)\Gamma(\xi)}\int_0^\tau x^{\eta-1}\Psi(x,\mathrm{X}(x))(\tau-x)^{\eta-1}dx+\frac{\eta(1-\xi)\tau^{\eta-1}\Psi(\tau,\mathrm{X}(\tau))}{\mathrm{AB}(\xi)}\right|\\&-\left|\mathrm{Z}(0)+\frac{\xi\eta}{\mathrm{AB}(\xi)\Gamma(\xi)}\int_0^\tau x^{\eta-1}\Psi(x,\mathrm{Z}(x))(\tau-x)^{\eta-1}dx+\frac{\eta(1-\xi)\tau^{\eta-1}\Psi(\tau,\mathrm{Z}(\tau))}{\mathrm{AB}(\xi)}\right|\\&\leq\varepsilon\xi_{\xi,\eta}^{*}+\mathrm{K}\left|\mathrm{X}(\tau)-\mathrm{Z}(\tau)\right|.\end{aligned}$$

Consequently,

$$\left\|\mathrm{X}(\tau)-\mathrm{Z}(\tau)\right\|\leq\varepsilon\mathrm{N}_{\xi,\eta},$$

where $\mathrm{N}_{\xi,\eta}=\dfrac{\xi_{\xi,\eta}^{*}}{1-\mathrm{K}}$. Hence, system (12) is U-H stable.

Consider the following perturbed solution of system (17):

$$\begin{cases} {}^{FFP}D_{0,\tau}^{\xi,\eta}\mathrm{X}(\tau) = \Psi(\tau, \mathrm{X}(\tau)) + \delta(\tau), \quad \tau \geq 0, \\ \mathrm{X}(0) = \mathrm{X}_0, \end{cases} \tag{26}$$

where $\delta(\tau) \in C[0,T]$.

Based on the above-mentioned analysis, system (26) fulfils the following inequality:

$$\left| \mathrm{X}(\tau) - \left(\mathrm{X}(0) + \frac{\eta}{\Gamma(\xi)} \int_0^\tau x^{\xi-1} \Psi(x, \mathrm{X}(x))(\tau - x)^{\xi-1} dx \right) \right| \leq \left(\frac{\eta T^{\xi+\eta-1} \beta(\xi,\eta)}{\Gamma(\xi)} \right) \varepsilon. \tag{27}$$

By similar analysis, the following lemma is straightforwardly proven.

Lemma 2. The U-H stability is demonstrated by C2 and the inequality (27). The solution of system (17) is U-H stable if $\left(\frac{\eta T^{\xi+\eta-1} \beta(\xi,\eta)}{\Gamma(\xi)} \right) L_a < 1.$

6. Numerical simulations of the 4D dynamical system under the FFDs

Throughout this section, the system's parameters are fixed at the following parameter sets $\alpha = -3, \beta = 15, \delta = -0.0001, \nu = -1.5, \sigma = 0.6.$ and $\alpha = -2, \beta = 15, \delta = -0.15, \nu = -7.775, \sigma = 0.45.$ Systems (12), (17), and (23) are numerically integrated based on the scheme given in [26].

6.1. Local stability of the equilibrium points

Using the parameter values $\alpha = -3, \beta = 15, \delta = -0.0001, \nu = -1.5, \sigma = 0.6$, systems (12), (17), and (23) are numerically integrated. The simulation results (See Figures 1 to 6) show that the non-origin equilibrium points ($\mathrm{P}_{1,2}$) of system (17) are LAS when the fractional-order and fractal dimension are below 0.7, simultaneously. In addition, the equilibrium points $\mathrm{P}_{1,2}$ of system (12) are LAS when the fractional-order is below 0.85 and fractal dimension is below 0.61, simultaneously. Furthermore, the equilibrium points $\mathrm{P}_{1,2}$ of system (23) are LAS when the fractional-order is below 0.78 and fractal dimension is below 0.01, simultaneously. Otherwise, they are not LAS.

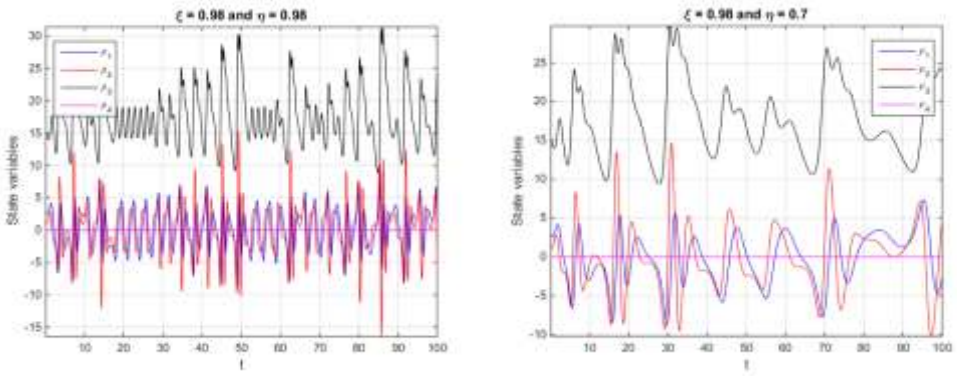

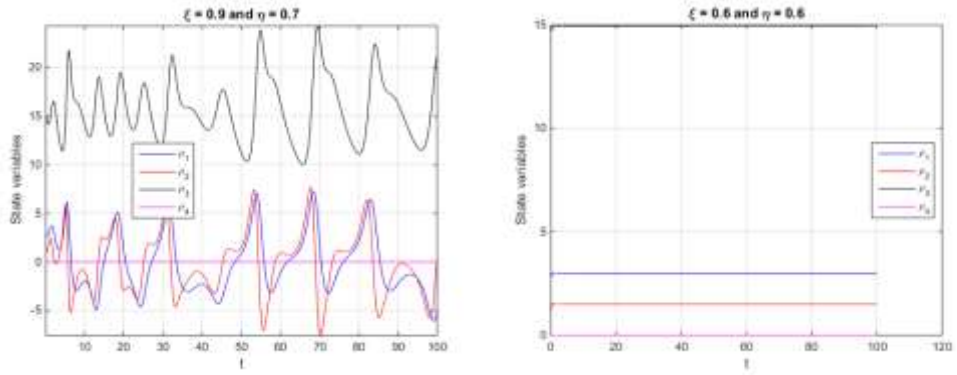

Figure 1. The plot of state variables of system (17) vs. time shows the local stability of $P_1 = (3,1.5,15,0)$ as ξ and η are changed.

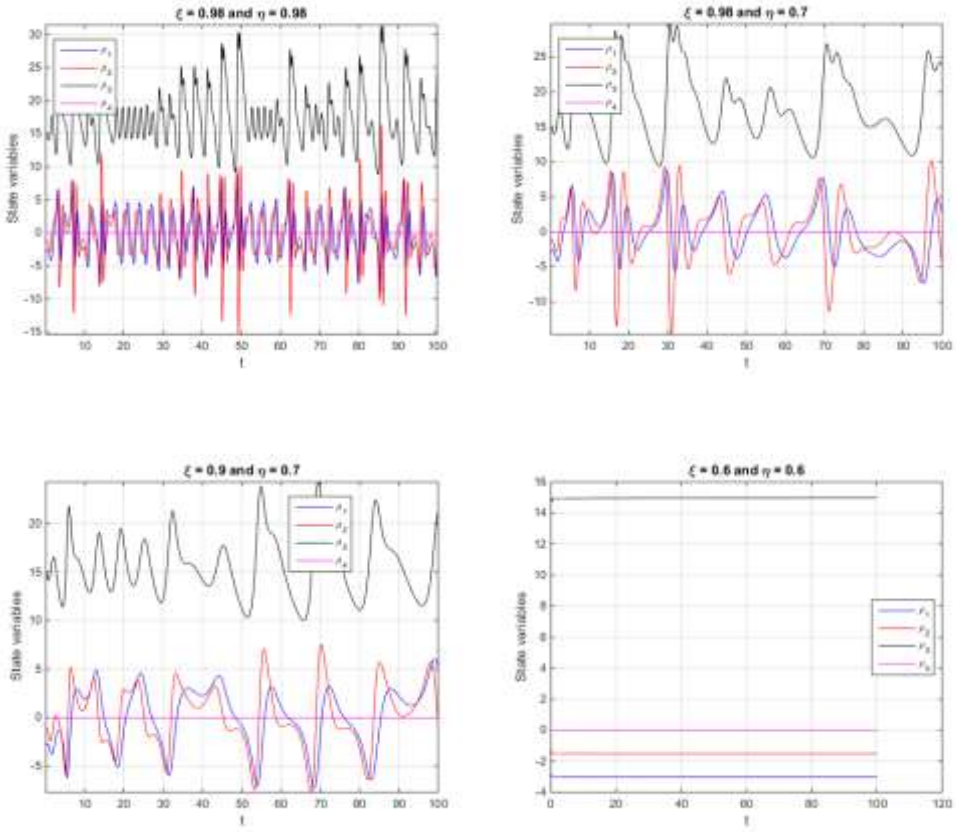

Figure 2. The plot of state variables of system (17) vs. time shows the local stability of $P_2 = (-3,-1.5,15,0)$ as ξ and η are changed.

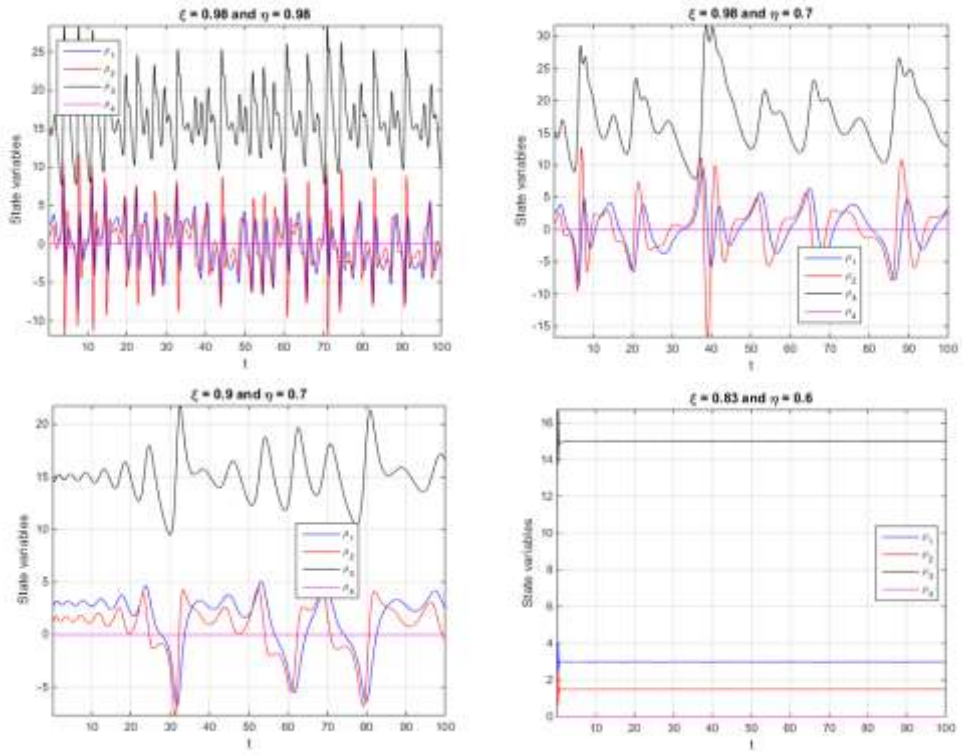

Figure 3. The plot of state variables of system (12) vs. time shows the local stability of $P_1 = (3,1.5,15,0)$ as ξ and η are changed.

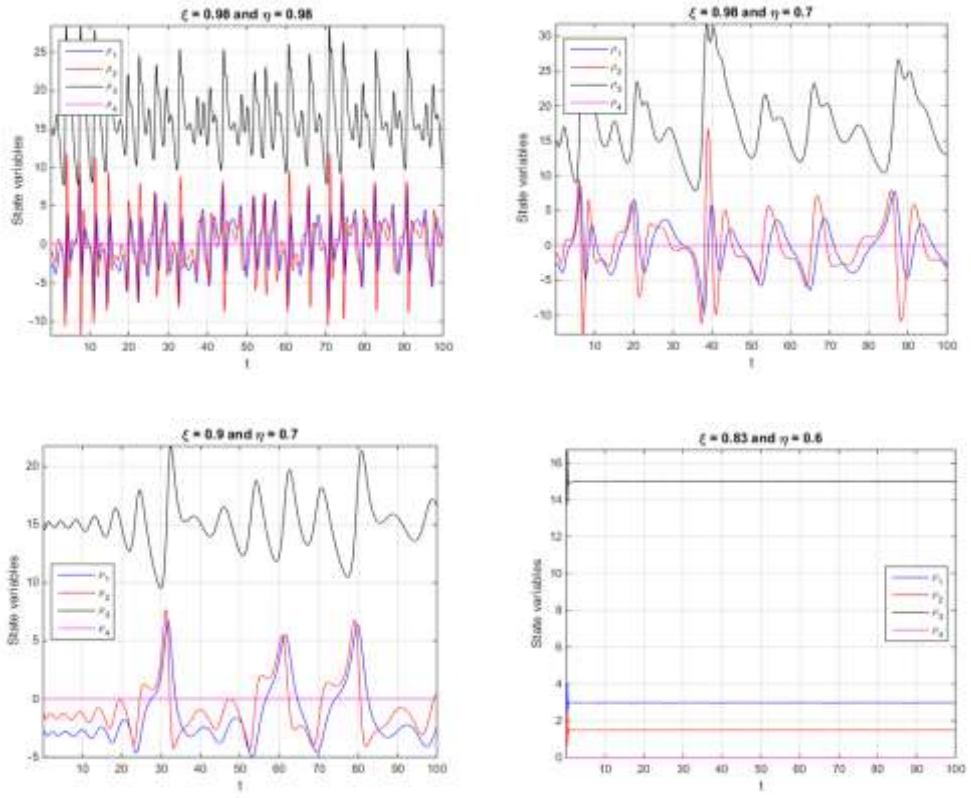

Figure 4. The plot of state variables of system (12) vs. time shows the local stability of $P_2 = (-3,-1.5,15,0)$ as ξ and η are changed.

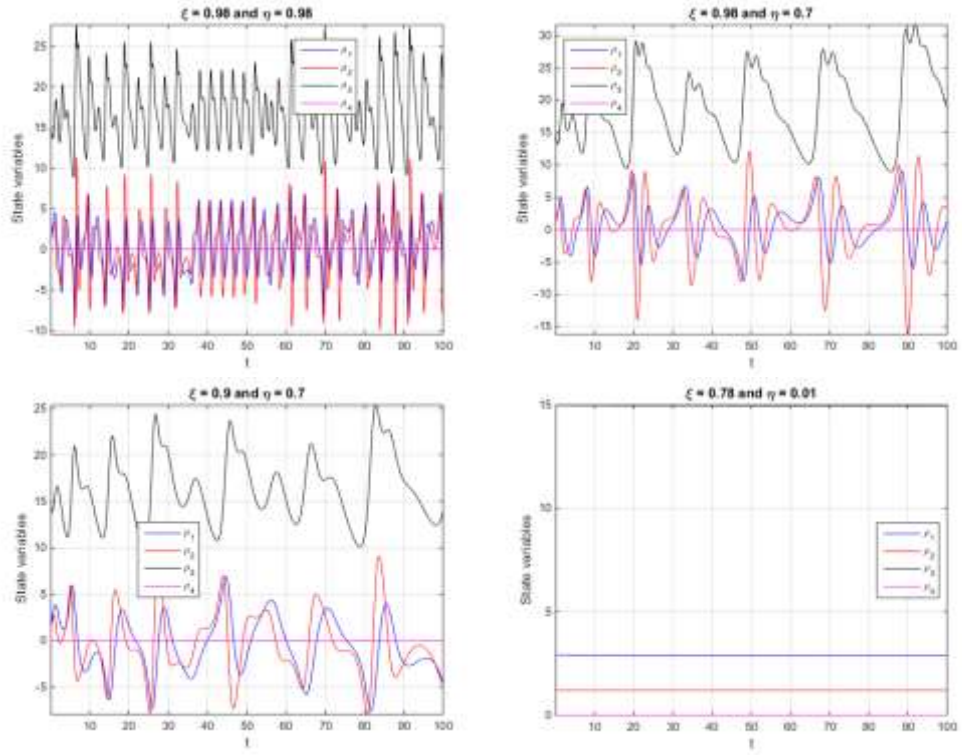

Figure 5. The plot of state variables of system (23) vs. time shows the local stability of $P_1 = (3,1.5,15,0)$ as ξ and η are changed.

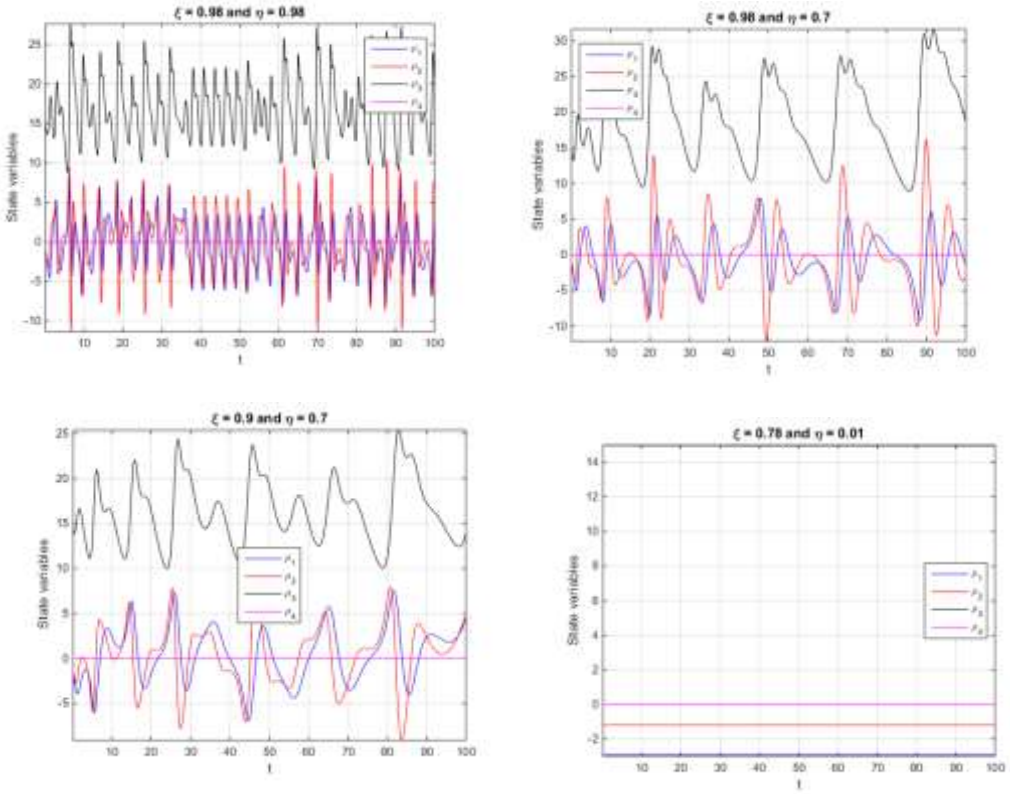

Figure 6. The plot of state variables of system (23) vs. time shows the local stability of $P_2 = (-3,-1.5,15,0)$ as ξ and η are changed.

For the parameter set $\alpha = -2, \beta = 15, \delta = -0.15, \nu = -7.775, \sigma = 0.45, \xi = 0.9975$ and $\eta = 0.99$, the points $P_1 = (2.598, 10.1, 15, 0)$ and $P_2 = (-2.598, -10.1, 15, 0)$ are LAS as shown in Figure 7.

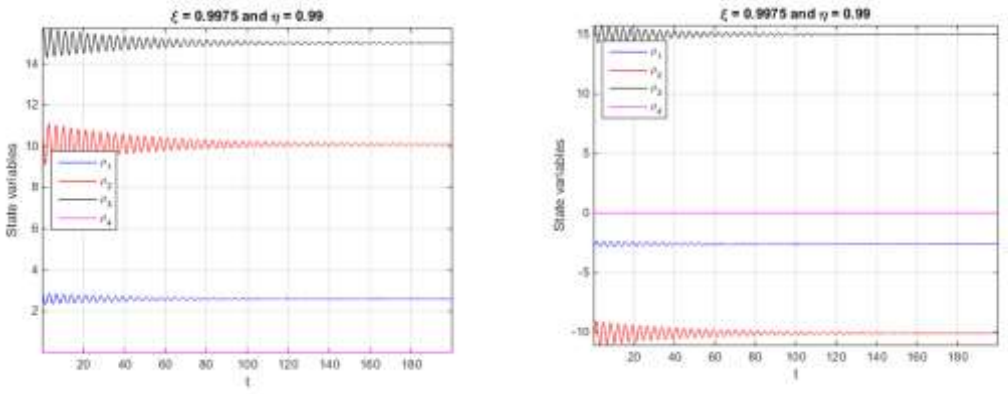

(a) (b)

Figure 7. The plot of state variables of system (23) vs. time shows the local stability of (a) $P_1 = (2.598, 10.1, 15, 0)$ and (b) $P_2 = (-2.598, -10.1, 15, 0)$.

6.2. Chaotic and hidden chaotic attractors

The attractors illustrated in the Figures 8 to 14 are obtained using step size of 0.01 and initial data $\rho_1(0) = 0, \rho_2(0) = 1, \rho_3(0) = 2, \rho_4(0) = 0.02$.

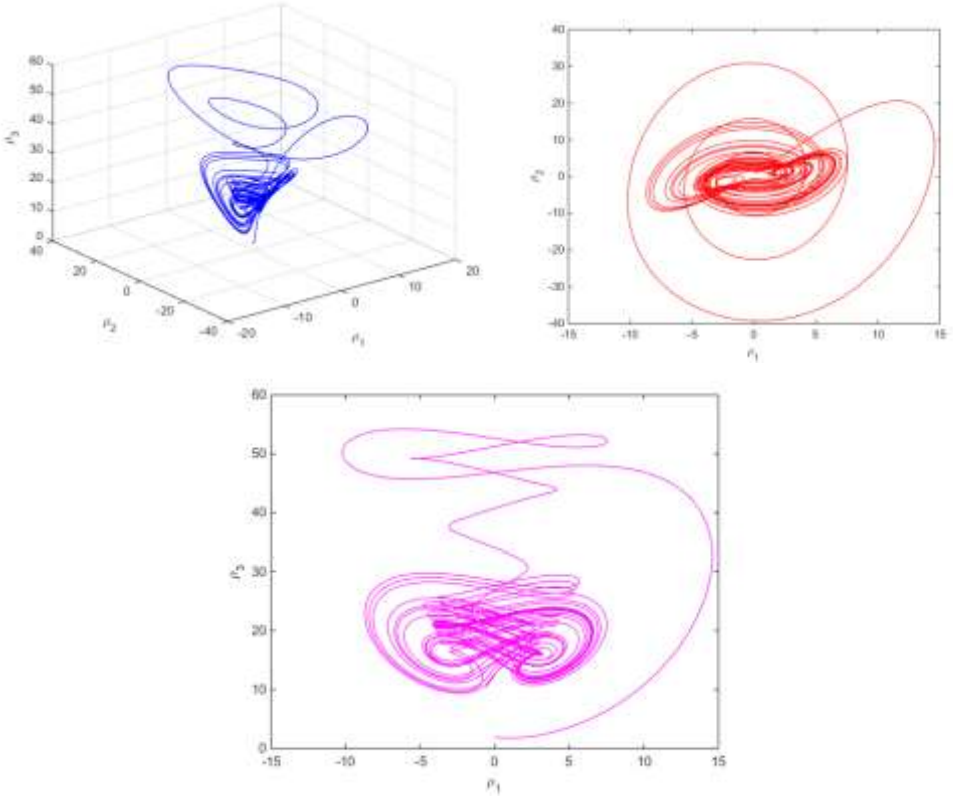

Figure 8. Chaotic dynamics in system (12) are shown when $\xi = 0.98$ and $\eta = 0.98$.

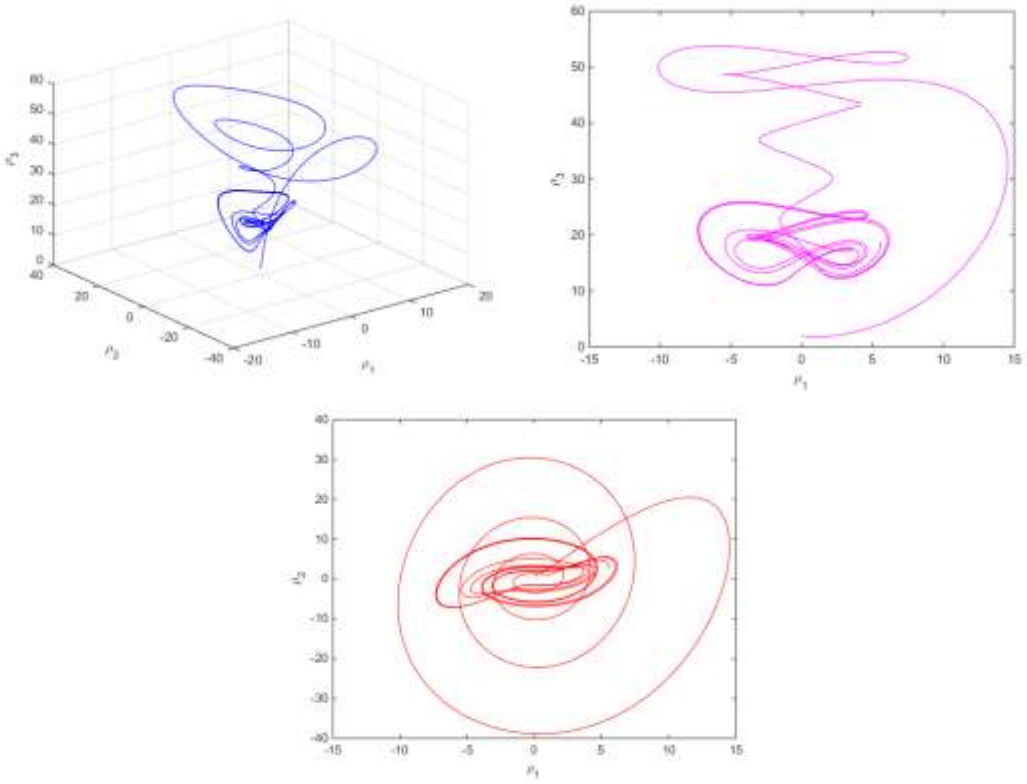

Figure 9. Complex dynamics in system (12) are shown when $\xi = 0.98$ and $\eta = 0.7$.

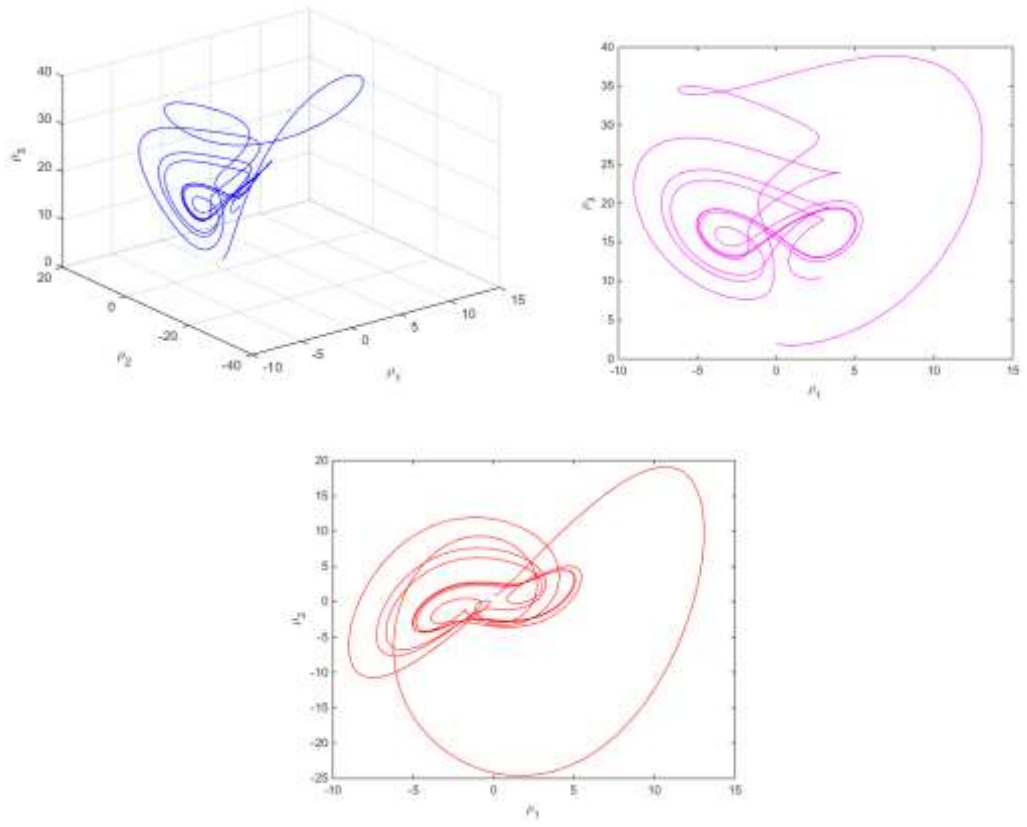

Figure 10. Complex dynamics in system (12) are shown when $\xi = 0.90$ and $\eta = 0.7$.

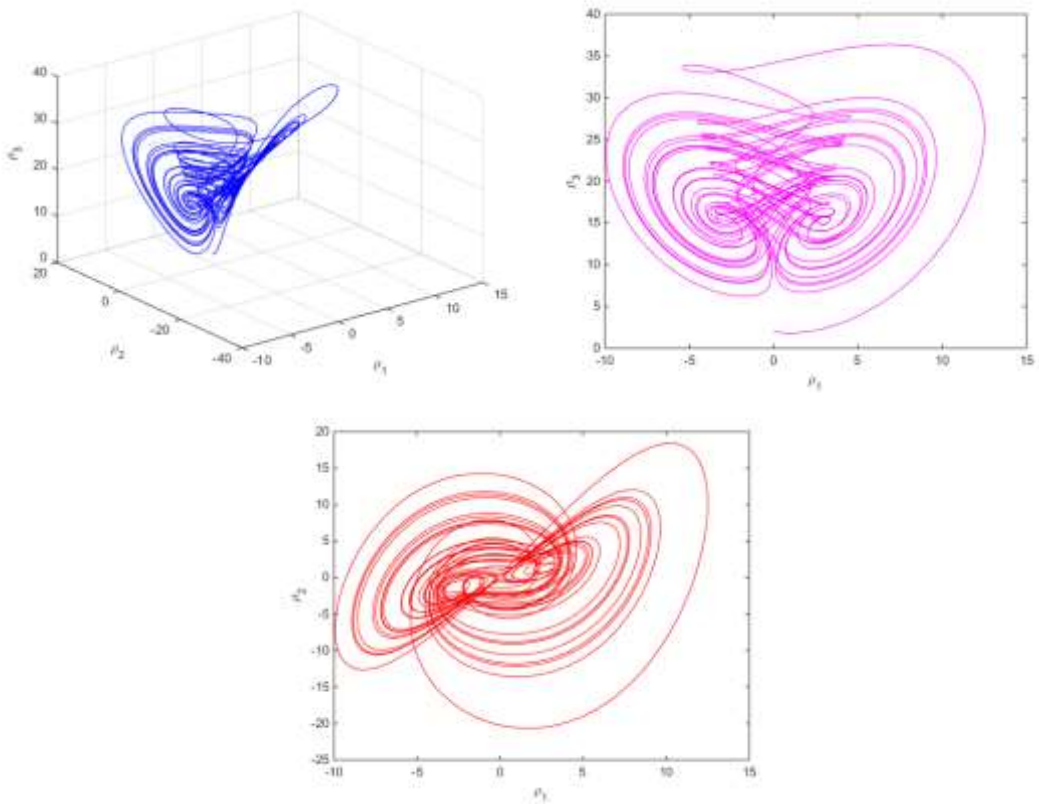

Figure 11. Chaotic dynamics in system (17) are shown when $\xi = 0.98$ and $\eta = 0.98$.

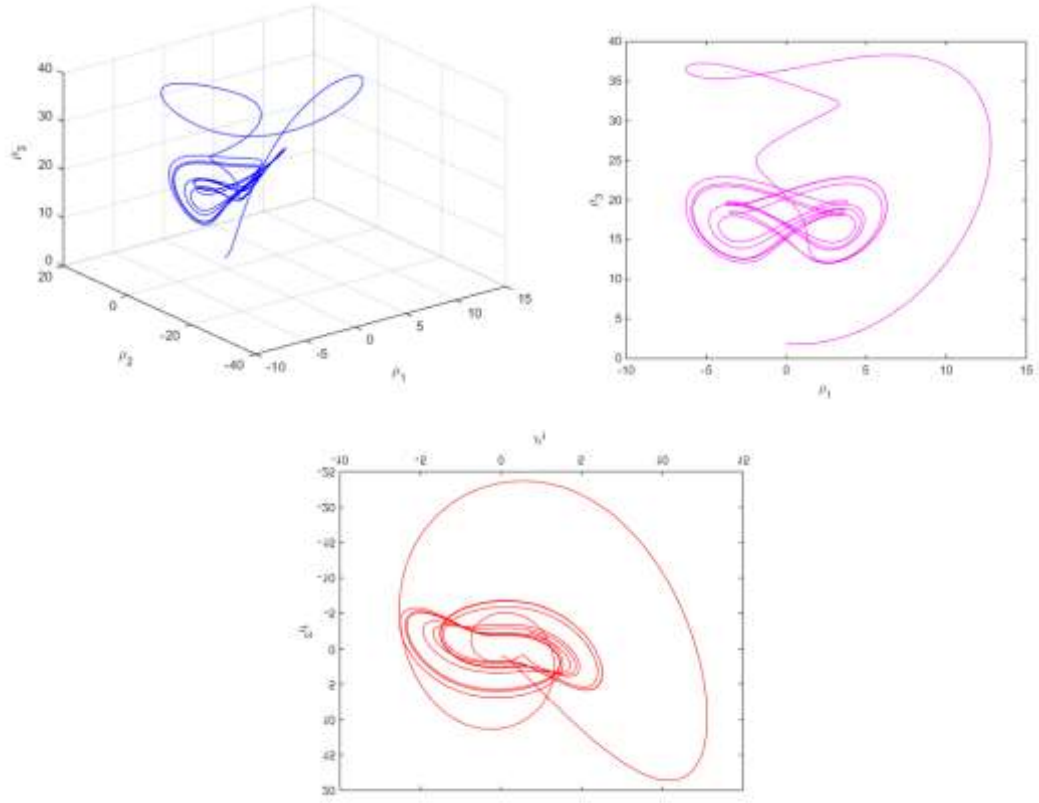

Figure 12. Complex dynamics in system (17) are shown when $\xi = 0.98$ and $\eta = 0.7$.

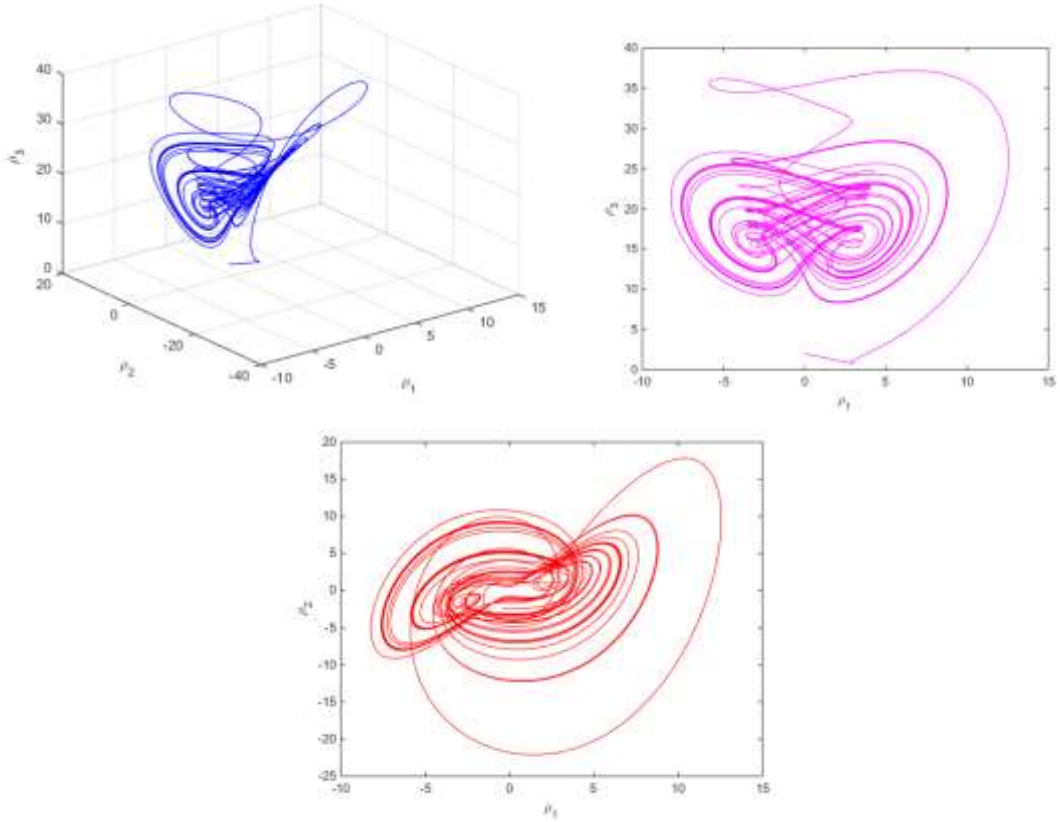

Figure 13. Chaotic dynamics in system (23) are shown when $\xi = 0.98$ and $\eta = 0.98$.

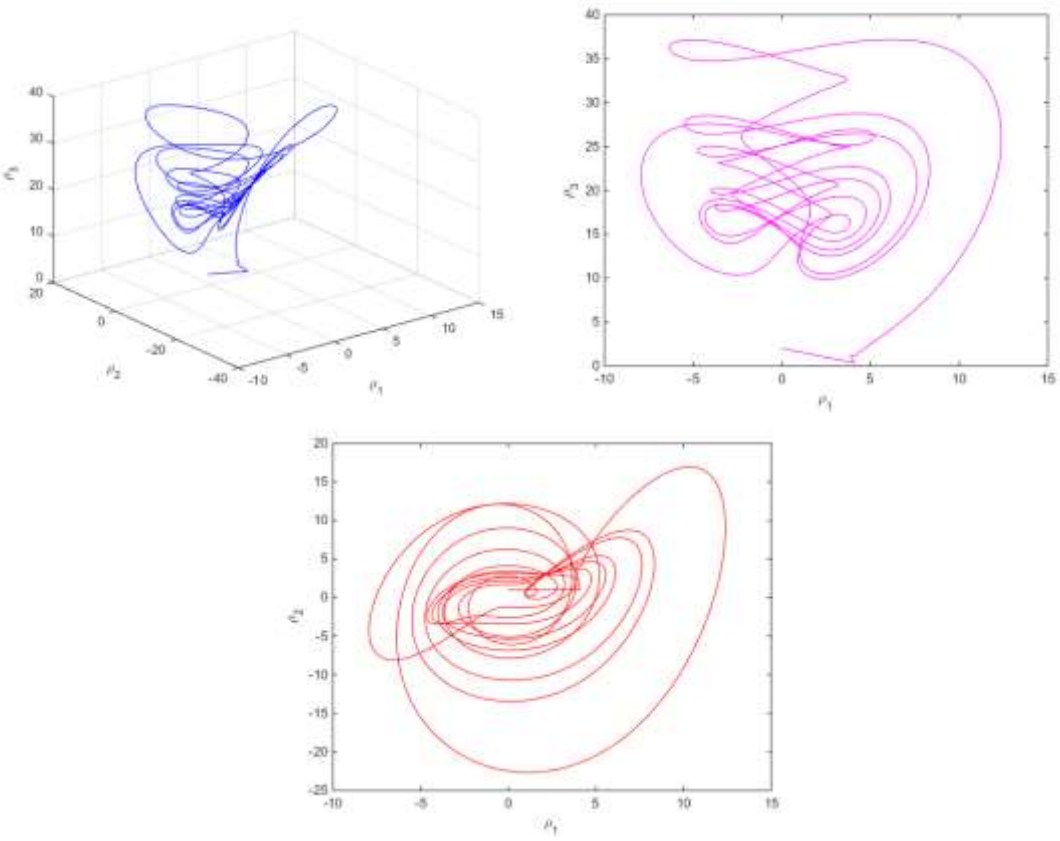

Figure 14. Complex dynamics in system (23) are shown when $\xi = 0.98$ and $\eta = 0.7$.

The systems' bifurcation diagrams are also carried out to compute their local maxima. Figures 15 to 17 show the bifurcation diagrams of systems (12), (17), and (23) as the fractional or fractal-fractional parameters are varied. These figures are helpful to illustrate the wide scale of chaotic dynamics that exist in these systems.

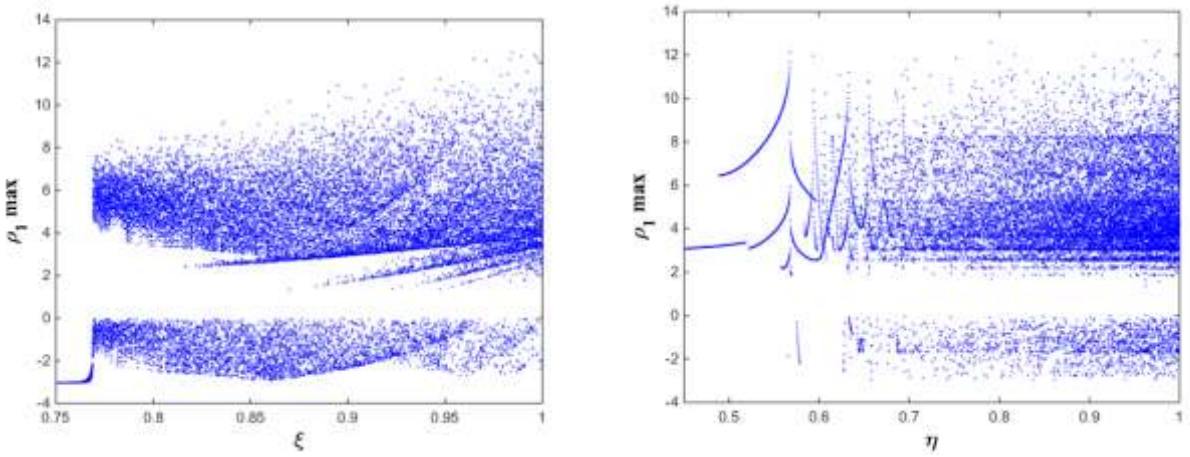

(a) (b)

Figure 15. The bifurcation diagram of system (17) as (a) ξ varies and (b) η varies.

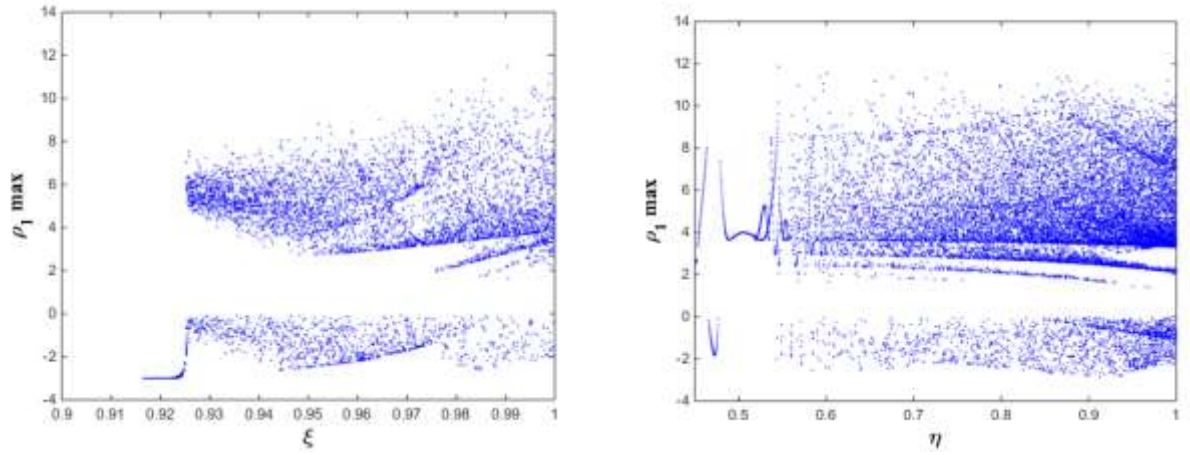

(a) (b)

Figure 16. The bifurcation diagram of system (12) as (a) ξ varies and (b) η varies.

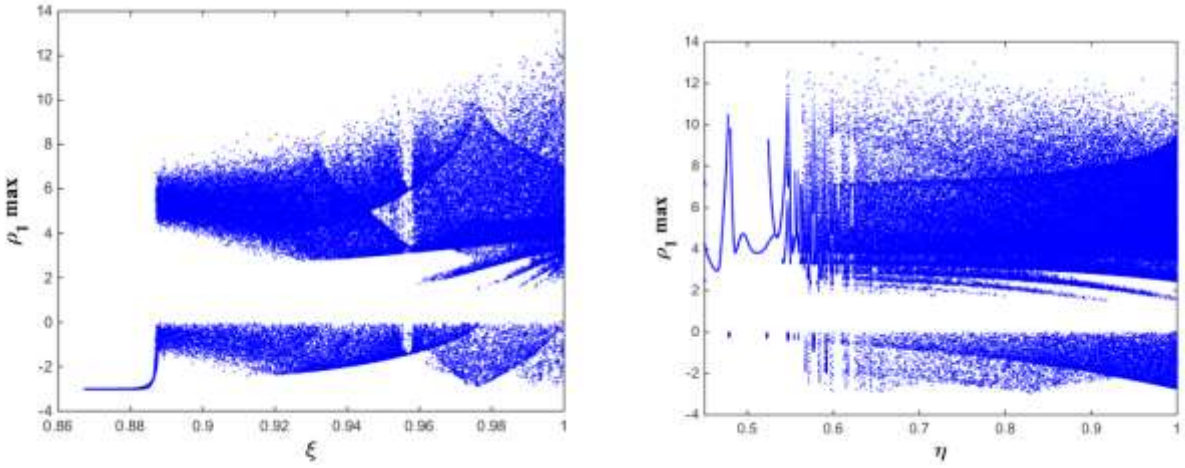

(a) (b)

Figure 17. The bifurcation diagram of system (23) as (a) ξ varies and (b) η varies.

The systems' LEs are calculated using the above-mentioned parameter values. The results are illustrated in Figures 18–20, showing show the variation of the maximal Lyapunov exponents (MLEs) against the parameter ξ or the parameter η. The previous figures show that chaotic dynamics continue to occur in these systems over relatively large ranges of fractional and fractal-fractional parameters.

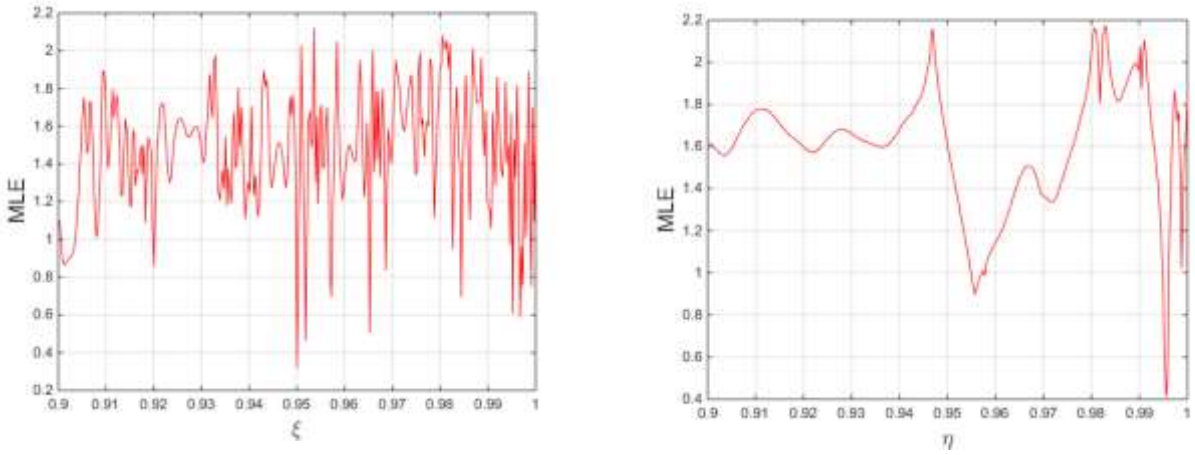

(a) (b)

Figure 18. The MLEs of system (17) as (a) ξ varies and (b) η varies.

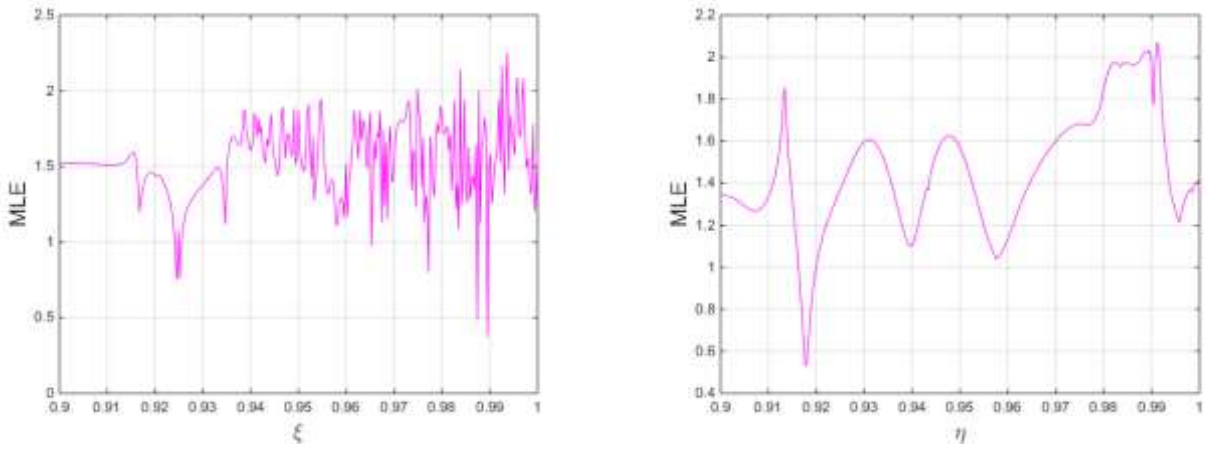

(a) (b)

Figure 19. The MLEs of system (12) as (a) ξ varies and (b) η varies.

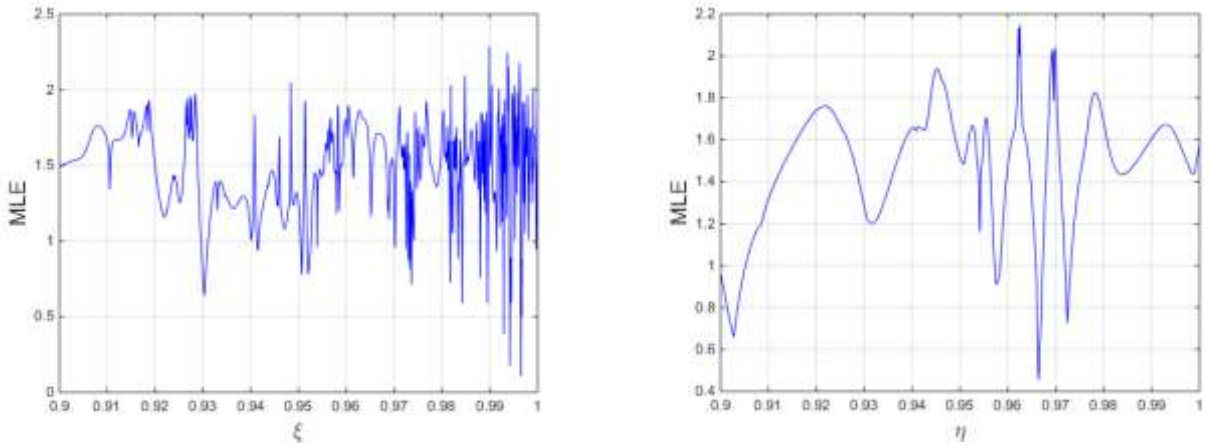

(a) (b)

Figure 20. The MLEs of system (23) as (a) ξ varies and (b) η varies.

On the other hand, hidden chaotic attractors are interesting dynamical phenomenon that exist in the considered system. This phenomenon is observed when any basin set of attraction of the hidden attractor does not touch small neighborhoods of any existing equilibrium point [27]. For example, when the Caputo-Fabrizio fractal-fractional operators are used, a hidden chaotic attractor appears for $\alpha = -2, \beta = 15, \delta = -0.15, \nu = -7.775, \sigma = 0.45, \xi = 0.9975$ and $\eta = 0.99$. The explanation is provided as follows: The LAS equilibrium points $\mathrm{P}_1 = (2.598, 10.1, 15, 0)$ ($\mathrm{P}_2 = (-2.598, -10.1, 15, 0)$) attract all trajectories emanating close enough to them (sinks). Thus, any chaotic attractor starting near the saddle origin equilibrium point that does not intersect the sinks would form the hidden attractor. In Figure 21, the green domain refers to the hidden chaotic attractor that is swinging between the positive and negative parts of the ρ_1 axis. In addition, this figure shows that the hidden chaotic attractor is surrounding, and not touching, the sinks, which converge to the non-origin equilibrium points. These sinks are represented by blue and red domains. The corresponding bifurcation diagrams and basin set of attraction are illustrated in Figures 22 and 23, respectively. The hidden chaos is visible through the green area at the top right of Figure 22. In Figure 23, the color bar illustrates the existence of the

multistability phenomenon as follows; the red domain refers to a hidden chaotic attractor, and the dark blue domain refers to another type of hidden chaos. The yellow domain refers to the one-point attractor related to $P_1 = (2.598,10.1,15,0)$, while the light blue domain refers to the one-point attractor related to $P_2 = (-2.598,-10.1,15,0)$. Finally, the green domain at the top left and bottom right of the Figure 23 refer to divergent attractors.

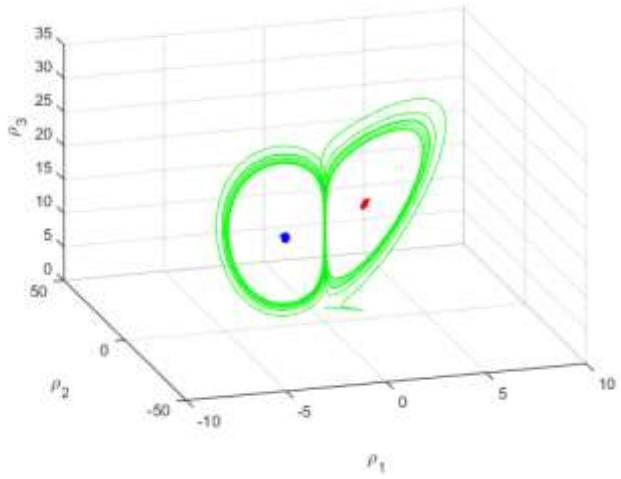

Figure 21. A hidden chaotic attractor of system (23).

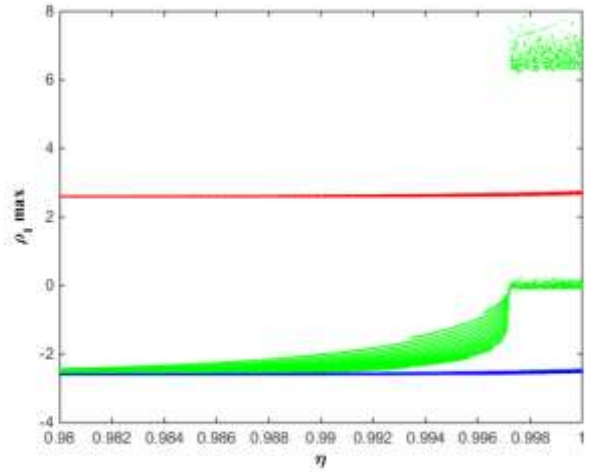

Figure 22. The combined bifurcation diagrams of system (23) as η varies.

The fixed parameters are at $\alpha = -2, \beta = 15, \delta = -0.15, \nu = -7.775, \sigma = 0.45$ and $\xi = 0.9975$. The green, red, and blue domains refer to the initial conditions $\rho_1(0) = 0, \rho_2(0) = 1, \rho_3(0) = 2, \rho_4(0) = 0.02,$ $\rho_1(0) = 2.7, \rho_2(0) = 10.6, \rho_3(0) = 15, \rho_4(0) = 0.0001$ and $\rho_1(0) = -2.7, \rho_2(0) = -10.6, \rho_3(0) = 15, \rho_4(0) = 0.0001$, respectively.

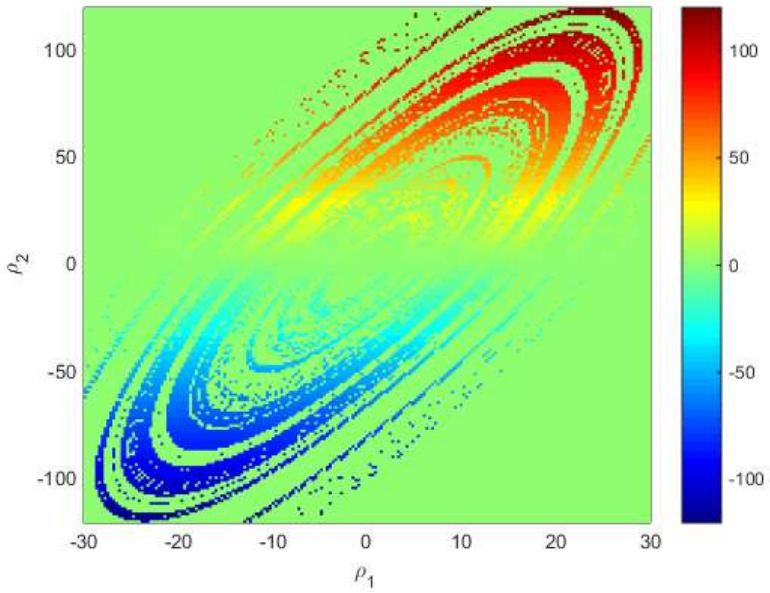

Figure 23. The attraction basin for system (23) as a cross-section in $\rho_1\rho_2-$plane for $\rho_3=15,\rho_4=0.0001,$ with $\alpha=-2,\beta=15,\delta=-0.15,\nu=-7.775,\sigma=0.45,\ \xi=0.9975$ and $\eta=0.99.$

7. Conclusions

In this work, the Caputo, Atangana-Baleanu, and Caputo-Fabrizio fractal-fractional operators have been applied to generate chaotic attractors and complex dynamics in a 4D dynamical system. Some conditions for the exact solutions' existence and uniqueness have been demonstrated when the fractal-fractional operators are implemented into the proposed system. Some U-H stability results have been demonstrated in the indicated fractal-fractional systems. Computation processes have been carried out to demonstrate some graphical results that show the existence of several complex dynamics in the considered system as the fractal-fractional operators are implemented. The MLEs have been depicted, and the corresponding bifurcation diagrams have been illustrated based on the systems' local maxima of a state variable to illustrate the wide scale of chaotic dynamics that exist in the considered systems. Finally, the basin set of attraction is computed to illustrate the interesting dynamical phenomenon of hidden chaotic attractors that exist in the considered system.

Investigating the conditions for local stability of a generalized fractal-fractional system will be studied in future works.

Conflict of interest

The author declares no conflicts of interest in this paper.

Acknowledgement

The author extends the appreciation to the Deanship of Postgraduate Studies and Scientific Research at Majmaah University for funding this research work through the project number (R-2025-1571).

Use of Generative-AI tools declaration

The authors declare they have not used artificial intelligence (AI) tools in the creation of this article.

References

1. G. Pertz, C. J. Gerhardt, *Briefwechsel zwischen Leibniz, Hugens van Zulichem und dem Marquis de l'Hospital*, Leibnizens gesammelte Werke*,* 1849.
2. M. Caputo, Linear models of dissipation whose Q is almost frequency independent-II, *Geophys. J. R. Astron. Soc.*, **13** (1967), 529–539. https://doi.org/10.1111/j.1365-246X.1967.tb02303.x
3. M. Caputo, M. Fabrizio, A new definition of fractional derivative without singular kernel, *Prog. Fract. Differ. Appl.*, **1** (2015), 73. http://dx.doi.org/10.12785/pfda/010201
4. A. Atangana, D. Baleanu, Caputo-Fabrizio derivative applied to groundwater flow within confined aquifer, *J. Eng. Mech.,* **143** (2017), D4016005. https://doi.org/10.1061/(ASCE)EM.1943-7889.0001091
5. A. Atangana, Fractal-fractional differentiation and integration: connecting fractal calculus and fractional calculus to predict complex system, *Chaos Soliton. Fract*., **102** (2017), 396–406. https://doi.org/10.1016/j.chaos.2017.04.027
6. C. Sparrow, *The Lorenz equations: Bifurcation, chaos and strange attractor*, New York: Springer-Verlag, 1982.
7. A. Wolf, J. B. Swift, H. L. Swinney, J. A. Vastano, Determining Lyapunov exponents from a time series, *Phys. D*, **16** (1985) 285–317.
8. E. N. Lorenz, Deterministic non-periodic flow, *J. Atmospheric Sci.,* **20** (1963), 130–141.
9. O. E. Rössler, An equation for continuous chaos, *Phys. Lett. A*, **57** (1976), 397–398.
10. A. E. Matouk, H. N. Agiza, Bifurcations, chaos and synchronization in ADVP circuit with parallel resistor, *J. Math. Anal. Appl.*, **341** (2008), 259–269. https://doi.org/10.1016/j.jmaa.2007.09.067
11. A. E. Matouk, Dynamics and control in a novel hyperchaotic system, *Int. J. Dyn. Cont.*, **7** (2019), 241. https://doi.org/10.1007/s40435-018-0439-6
12. I. Grigorenko, E. Grigorenko, Chaotic dynamics of the fractional Lorenz system, *Phys. Rev. Lett.*, **91** (2003), 034101. https://doi.org/10.1103/PhysRevLett.91.034101
13. W. Zhang, S. Zhou, H. Li, H. Zhu, Chaos in a fractional-order Rössler system, *Chaos Soliton. Fract.*, **42** (2009), 1684–1691. https://doi.org/10.1016/j.chaos.2009.03.069
14. A. E. Matouk, Chaos, feedback control and synchronization of a fractional-order modified autonomous Van der Pol-Duffing circuit, *Commun. Nonlinear Sci. Numer. Simulat.*, **16** (2011), 975–986. https://doi.org/10.1016/j.cnsns.2010.04.027
15. A. E. Matouk, A novel fractional-order system: Chaos, hyperchaos and applications to linear control, *J. Appl. Comput. Mech.*, **7** (2021), 701–714. https://doi.10.22055/JACM.2020.35092.2561
16. S. Qureshi, A. Atangana, Fractal-fractional differentiation for the modeling and mathematical analysis of nonlinear diarrhea transmission dynamics under the use of real data, *Chaos Soliton. Fract.*, **136** (2020), 109812. https://doi.org/10.1016/j.chaos.2020.109812

17. A. Sami, A. Ali, R. Shafqat, N. Pakkaranang, M. Rahmamn, Analysis of food chain mathematical model under fractal fractional Caputo derivative, *Math. Biosci. Eng.,* **20** (2022), 2094–2109. https://doi.org/10.3934/mbe.2023097
18. N. Almutairi, S. Saber, H. Ahmad, The fractal-fractional Atangana-Baleanu operator for pneumonia disease: Stability, statistical and numerical analyses, *AIMS Math.,* **8** (2023), 29382–29410. https://doi.org/10.3934/math.20231504
19. M. Arif, P. Kumam, W. Kumam, A. Akgul, T. Sutthibutpong, Analysis of newly developed fractal-fractional derivative with power law kernel for MHD couple stress fluid in channel embedded in a porous medium, *Sci. Rep.,* **11** (2021) 20858. https://doi.org/10.1038/s41598-021-00163-3
20. A. Khan, K. Shah, T. Abdeljawad, I. Amacha, Fractal fractional model for tuberculosis: existence and numerical solutions, *Sci. Rep.,* **14** (2024) 12211. https://doi.org/10.1038/s41598-024-62386-4
21. K. Shah, T. Abdeljawad, On complex fractal-fractional order mathematical modeling of CO2 emanations from energy sector, *Phys. Scripta,* **99** (2024) 015226. https://doi.org/10.1088/1402-4896/ad1286
22. A. Dlamini, E. F. D. Goufo, M. Khumalo, On the Caputo-Fabrizio fractal fractional representation for the Lorenz chaotic system, *AIMS Math.*, **6** (2021) 12395–12421. https://doi.org/10.3934/math.2021717
23. I. Ul Haq, N. Ali, H. Ahmad, Analysis of a chaotic system using fractal-fractional derivatives with exponential decay type kernels, *Math. Model. Control*, **2** (2022) 185–199. https://doi.org/10.3934/mmc.2022019
24. S. Saber, Control of chaos in the Burke-Shaw system of fractal-fractional order in the sense of Caputo-Fabrizio, *J. Appl. Math. Comput. Mech*., **23** (2024) 83–96. https://doi.org/10.17512/jamcm.2024.1.07
25. A. Granas, J. Dugundji, *Fixed point theory*, New York: Springer, 2005.
26. A. Atangana, S. Qureshi, Modeling attractors of chaotic dynamical systems with fractal-fractional operators, *Chaos Soliton. Fract.*, **123** (2019), 320–337. https://doi.org/10.1016/j.chaos.2019.04.020
27. N. V. Kuznetsov, G. Leonov, Hidden attractors in dynamical systems: systems with no equilibria, multistability and coexisting attractors, *IFAC Proc.*, **47** (2014), 5445–5454. https://doi.org/10.3182/20140824-6-ZA-1003.02501